Bioorganic & Medicinal Chemistry Letters xxx (xxxx) xxx–xxx

Contents lists available at ScienceDirect

Bioorganic & Medicinal Chemistry Letters

journal homepage: www.elsevier.com/locate/bmcl

Novel, potent, selective and brain penetrant vasopressin 1b receptor antagonists

Hervé Geneste[a,*], Swati Bhowmik[a,c], Marcel M. van Gaalen[a,c], Wilfried Hornberger[a], Charles W. Hutchins[b], Astrid Netz[a], Thorsten Oost[a,c], Liliane Unger[a,c]

[a] AbbVie Deutschland GmbH & Co. KG, Neuroscience Research, D-67008 Ludwigshafen, Germany
[b] AbbVie, Structural Biologie, IL 60064-6101, USA

ARTICLE INFO

Keywords:
Vasopressin 1b
V1b
SSR149415
Oxindole

ABSTRACT

Herein we report the discovery of a novel oxindole-based series of vasopressin 1b (V1b) receptor antagonists. Introducing a substituted piperazine moiety and optimizing the southern and the northern aromatic rings resulted in potent, selective and brain penetrant V1b receptor antagonists. Compound **9c** was found to be efficacious in a rat model of anti-depressant activity (3 mg/kg, ip). Interestingly, both moderate terminal half-life and moderate bioavailability could be achieved despite sub-optimal microsomal stability.

Vasopressin (AVP) is an endogenous hormone which exerts a large number of effects on organs and tissues. For example, it has been shown that a selective antagonist of the vasopressin Vlb receptor exerts anxiolytic- and antidepressant-like effects in animal models.[1] Vlb receptor antagonism is thus of particular interest for the treatment of affective disorders such as general anxiety disorders and major depression.

In particular oxindole SSR149415 was the first potent, selective, orally-active vasopressin V1b receptor antagonist disclosed (Fig. 1) to enter clinical trial for depression and anxiety; it was however discontinued later on due to extensive first-pass metabolism leading to sub-optimal pharmacokinetic properties (esp. short half-life).[2,3]

In a former publication,[4] we reported that metabolism occurs mainly by *N*-demethylation of the proline *N*,*N*-dimethylamide moiety. We want to present now our attempt to stabilize the metabolically susceptible residue by rigidification in a pipe-razin(on)e ring (Fig. 2).

A model for the V1b receptor was developed using homology modeling methodology starting from the crystal structure of the μ-opioid receptor.[5] This receptor was picked as the template since the identity was the highest (27%).[5] The receptor model was minimized for hundred steps of conjugate gradient minimization using Discover.[5]

Replacement by a piperazinone ring was supported by modeling (Fig. 3A); however the carbonyl of the formed piperazinone would rather overlap with the hydroxyl group carried by the proline moiety (Fig. 3A) contrary to our intuition and what is suggested by Fig. 2 (red dotted line); in other words it should rather be seen as a ring enlargement (5- to 6-membered ring) rather than as a cyclization. This hydroxyl group seems to be indeed key for the interaction of SSR149415 with a glutamine residue (Gln114) of the V1b receptor, whereas the carbonyl of the *N*,*N*-dimethylamide moiety might not contribute much to the interaction with the receptor (Fig. 3A). As suggested in Fig. 3A, two more residues (Lys111 and Gln168) induce strong interactions with the ligand involving the *o*-OMe substitutent and one oxygen atom of the sulfonamide function.

The 2-methoxypyridin-3-yl analog (**3b**[4]) was selected as starting point for this effort as it combines reduced overall lipophilicity, nanomolar binding to the human vasopressin 1b (hV1b) and selectivity towards the closely related vasopressins 1a and 2 (hV1a and hV2) and oxytocin (hOT) (s. discussion[4]). First derivatives (Table 1) were highly attractive, because of their significantly decreased molecular weight (< 600) and reduced in vitro microsomal clearance (compounds **3c** & **3d**, Table 1). However, they achieved far lower LLE[6] (8.5 down to 4.7 & 5.2, resp.) due to their dramatically diminished hV1b binding affinity (K_i 1.3 & 0.2 μM, resp.). The best combination (lower MW of 601 and best in vitro potency of 41 nM, compound **3f**) was obtained after additional substitution (methylation) and chiral separation[7]; alternatively piperazinone *N*-substitution with a 3-pyridin residue was also shown to be beneficial for V1b potency (K_i 82 nM, compound **3e**). According to our V1b model, replacing the terminal methyl substituent (in **3d**) by a pyridine moiety (in **3e**) might introduce additional favorable Π-stacking interactions with 2 phenylalanine residues (Phe 297 and 320, Fig. 3B).

These analogs were synthesized[8] by addition of the lithiated heterocycle[9] to 5-chloroisatin (Scheme 1). After chlorination in the 3-

* Corresponding author.
E-mail address: herve.geneste@abbvie.com (H. Geneste).
[c] S.B., M.v.G., T.O. and L.U. are former AbbVie/Abbott employees.

https://doi.org/10.1016/j.bmcl.2018.07.043
Received 20 June 2018; Received in revised form 26 July 2018; Accepted 29 July 2018

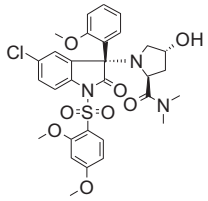

Fig. 1. SSR149415 (absolute configuration according to literature ref.[1]).

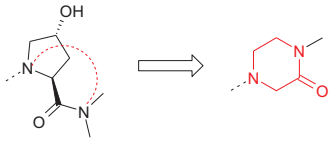

Fig. 2. Rigidification of the proline *N*,*N*-dimethylamide moiety.

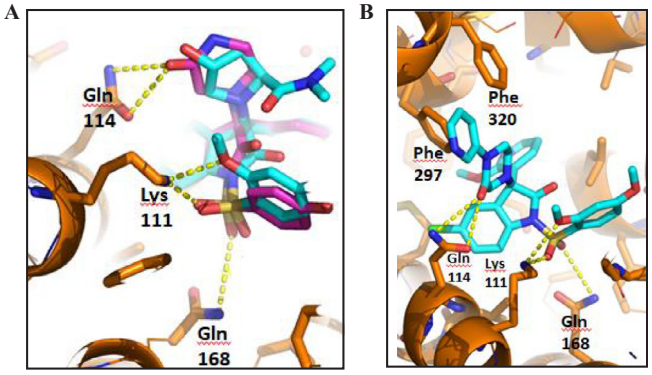

Fig. 3. A) Compounds **3c** & **3b** (in stick presentation, magenta and cyan, resp.) in the V1b model. B) Compound **3e** in the V1b model. [Residues of protein in stick presentation are within a distance of 6 Å around the molecule. The yellow dotted lines highlight the interactions with the receptor.]

Table 1
Receptor profile[a] and metabolic stability[b] of analogs **3b** to **3f**.

Compds	hV1b K_i, nM	V_{1a}/V_{1b}	OT/V_{1b}	Microsomal stability mCl, µL/min/mg	
				human	rat
3b[4]	1.3	42	32	323	446
3c	1340				
3d	192			99	113
3e	82	1	0	196	291
3f[c]	41	1	0	51	78

[a] hV1b K_i, hV1a K_i and hOT K_i values were determined according to literature procedures[10] and are means of at least two experiments (MSR[10] 2.8). Selectivities vs hV1a and hOT are calculated as follows: K_i hV1a/ K_i hV1b and K_i hOT/ K_i hV1b resp.

[b] Microsomal intrinsic clearance values (mCl) were determined according to literature procedures[11] and are means of at least two experiments.

[c] Active diastereomer.[7]

position with thionyl chloride, the amine moiety was introduced via nucleophilic substitution. Final compounds were obtained by sulfonylation with 2,4-dimethoxyphenylsulfonyl chloride. Eventually stereoisomers were either separated after the amination or after the sulfonylation stage.

Gratifyingly the piperazine analog (**4a**, Table 2, Fig. 4), synthesized from commercially available 4-pyridin-piperazine depicted comparable hV1b potency but improved metabolic stability despite higher lipophilicity (clogP 4.0, compared to 2.6 for compound **3e**).[12]

Encouraged by this result, more piperazine analogs were prepared (Table 2, Fig. 4). Replacement of the northern 2-methoxypyridin3-yl

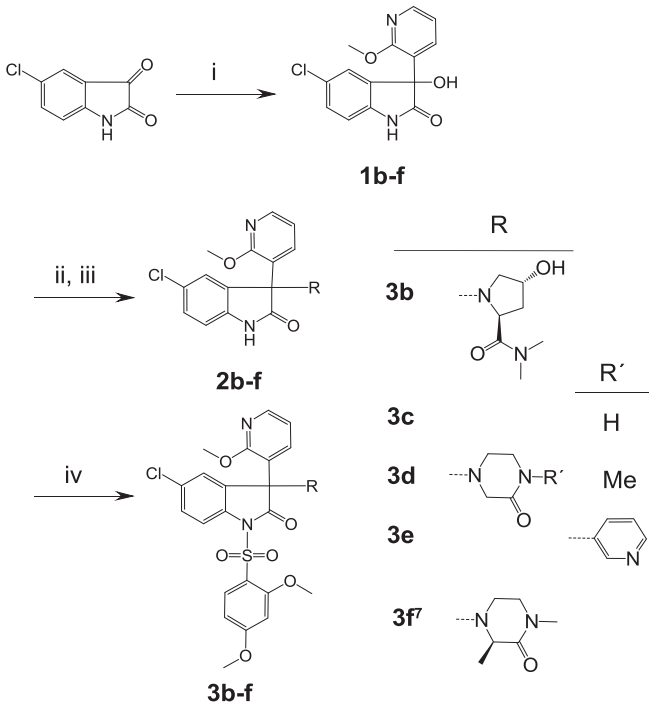

Scheme 1. Synthesis[8] of analogs **1b–f** and **3b–f**: (i) bromomesitylene, *tert*-butyllithium, 2-methoxypyridine, 20%; (ii) $SOCl_2$, pyridine, CH_2Cl_2, crude; (iii) amine RH, DIPEA, CH_2Cl_2/THF; (iv) NaH, DMF, sulfonyl chloride. Separation[8] of diastereomers after (iii) or (iv).

Table 2
Receptor profile[a] and metabolic stability[b] of analogs **4a** to **4f**.

Compds (Fig. 4)	hV1b K_i, nM	V_{1a}/V_{1b}	OT/V_{1b}	Microsomal stability mCl, µL/min/mg	
				human	rat
4a	45	0.1		19	84
4b	18	0.8	0.9	41	348
4c	233				
4d	47			93	442
4e	104				
4f	8	3	10	360	359

[a,b] *cf.* Table 1.

moiety by a 2-methoxyphenyl moiety (compound **4b**) improved further the hV1b potency (K_i 18 nM). In our attempt to reduce the molecular weight by removing one substituent carried by the southern phenyl ring we experienced loss of in vitro potency (compounds **4c**, **4d** & **4e**, Fig. 5).

Our V1b model (Fig. 5) suggested that the *p*-OMe substituent did not contribute much to the biological activity (compare analogs **4c** & **4e,** K_i 233 & 104 nM resp.). On the contrary the *o*-OMe substituent (compare analogs **4c** & **4d,** K_i 233 & 47 nM resp.) interacted with a lysine residue (Lys111) of the protein (Fig. 5).

Out of a library of > 20 variations (data not shown) only the 8-quinoline residue (compound **4f**) yielded a single digit nM potent compound (K_i 8 nM). Unfortunately microsomal intrinsic clearance (mCl) as well as selectivity towards related receptors (hV1a & hOT, < 10-fold) were poor.

The diminution of the overall lipophilicity[13] was investigated as an approach to address the high metabolism (Table 3, Fig. 3). The northern phenyl moiety was thus replaced by a 3-pyridinyl residue (compound **5a**) and the 5-chloro substituent by a 5-cyano (compound **5b**) in order to introduce higher polarity.[14]

These derivatives were synthesized[8] by addition of the lithiated

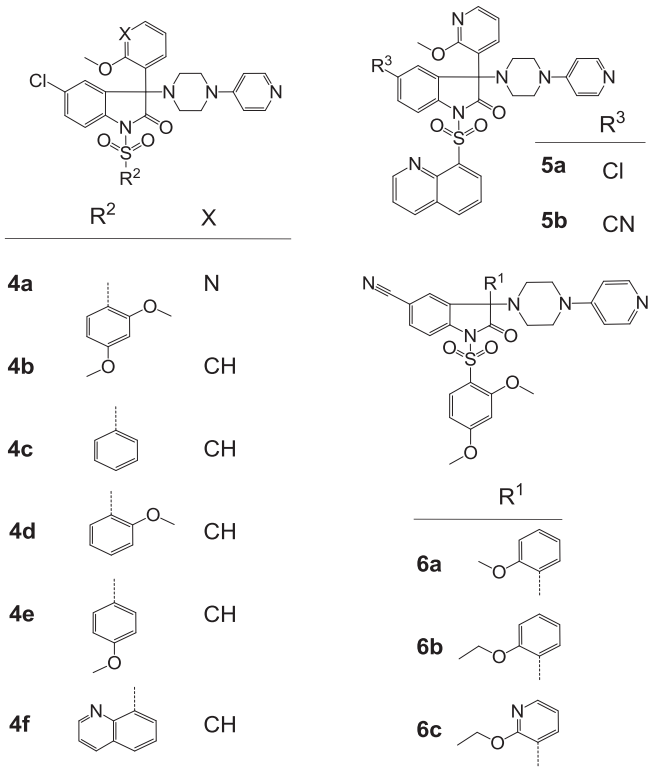

Fig. 4. Derivatives **4a–f**, **5a–b** & **6a–c**.

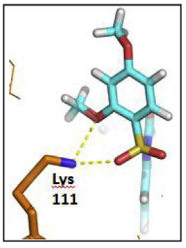

Fig. 5. Compound **4a** southern substituted phenyl (in stick presentation) in the V1b model. [Residues of protein in stick presentation are within a distance of 6 Å around the molecule. The yellow dotted lines highlight the interactions with the receptor.]

Table 3
Receptor profile[a] and metabolic stability[b] of analogs **5a and b** & **6a–c**.

Compds (Fig. 4)	hV1b K_i, nM	V_{1a}/V_{1b}	OT/V_{1b}	Microsomal stability mCl, µL/min/mg	
				human	rat
5a	15.2	0.5	2	554	156
5b	30.2	0.9	3	326	113
6a	58.5			43	296
6b	36			43	83
6c	84			77	168

[a,b] *cf.* Table 1.

heterocycle[9] to 5-iodoisatin (Scheme 2).[15] The high yielding iodo to cyano exchange occured subsequently by palladium (II) catalyzed reaction with $Zn(CN)_2$.[8]

The significant lowering effect on clogP (from 4.3 to 2.5) didn't impact very much the microsomal clearance which remained too high (s. analogs **4f** vs **5b**, Tables 2 and 3 resp.). Nevertheless as we felt that lower lipohilicity would be beneficial for future PK profiles, a focus was put on the 5-cyano series. Compound **6a** which offered a promising

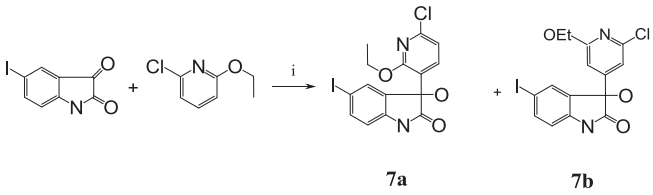

Scheme 2. Synthesis[8] of intermediate **7a**: (i) bromomesitylene, *tert*-butyllithium, 2-chloro-6-ethoxypyridine, 40%, 7a:7b 1:1 to 3:1.[15]

balance of biological activity and metabolic stability was chosen as starting point (hV1b K_i 59 nM, and moderate hmCl 43 µl/min/mg). Methoxy elongation to ethoxy (analog **6b**, northern phenyl ring, clogP 3.9) had a favorable effect on rmCl (83 µl/min/mg). However reducing further the clogP (3.3, compound **6c**, northern pyridine moiety) was detrimental to both potency and microsomal clearance.

We then looked at disubstitution of the northern ring, in particular 2,4- and 2,5-disubstitution (Tables 4 and 5, Fig. 6); in order to expedite our investigation, this effort was guided both by in-house collected SAR within related chemical series (data not shown) as well as by commercial availability of building blocks.

Introducing an additional methoxy substituent in the 4-position (compound **8a**, Table 4, Fig. 6) had a very favorable effect on the hV1b potency but also on both the microsomal stability and the selectivity towards V1a (34-fold). When moving to 2,4-disubstituted pyridins (compound **8b**), a remarkable metabolic stability (esp. in rat microsomes) could be achieved however accompanied by some loss of binding affinity.

We discussed earlier the potential interaction of the *o*-methoxy substituent carried by the southern phenyl moiety to a lysine residue (Lys111, Fig. 5). Indeed replacement of the latter substituent by a nitrogen in the ring is tolerated [compare analogs **8b** & **8d** (Table 4, Fig. 6), and analogs **9b** & **9f** (Table 5, Fig. 6)]. As suggested by our model (Fig. 7), the ring nitrogen could induce an interaction to Lys111 mediated by a water molecule as well as a boost in biological activity (e.g. improved in vitro hV1b potency of analog **8b** (K_i 45 nM) to analog **8d** (K_i 1 nM)). Finally the high contribution of the nitrogen atom to the biological activity is supported by the low potency of analog **9 g** when both ring nitrogen and *o*-methoxy are absent (Table 5, Fig. 6).

Analog **(+)-8c**[16] achieved the best profile in this series combining sub-nM V1b potency, high selectivity (> 50-fold towards V1a, OT), high microsomal stability and favorable PK profile and brain penetration in rat (F 37%, Cl_p 0.9 l/h/kg, b/p 1.0, Table 6). Compared to analog **8d** (the de-methylated analog), introduction of a methyl group had no impact on V1b affinity, slightly disfavored V1a & OT selectivity but contributed significantly to microsomal stability. As we had anticipated, the introduction of a methyl group in alpha position to the nitrogen of the pyridine ring (of the side chain) decreased the CYP3A4 inhibitory activity[17]; this is a case of steric shielding, hindering the CYP interaction and thus limiting microsomal metabolism.[18]

Comparable effects were observed in the 2,5-disubsted sub-series

Table 4
Receptor profile[a] and metabolic stability[b] of analogs **8a–d**.

Compds (Fig. 6)	hV1b K_i, nM	V_{1a}/V_{1b}	OT/V_{1b}	Microsomal stability mCl, µL/min/mg	
				human	rat
8a	10	34	3	63	34
8b	45			23	0
(±)-8c	1.3	125	69	–	–
(+)-8c[c]	0.9	78	65	7	22
8d	1.1	325	201	39	63

[a,b] *cf.* Table 1.
[c] Active enantiomer.[16]

Table 5
Receptor profile[a] and metabolic stability[b] of analogs **9a–g**.

Compds (Fig. 6)	hV1b K_i, nM	V_{1a}/V_{1b}	OT/V_{1b}	Microsomal stability mCl, µL/min/mg	
				human	rat
9a	13	2	2	50	58
9b	21	21	6	23	41
9c	5	79	34	170	210
9d	2	84	4	33	15
9e	9	39	21	131	119
9f	2	216	230	45	290
9g	32		15	93	118

[a,b] *cf.* Table 1.

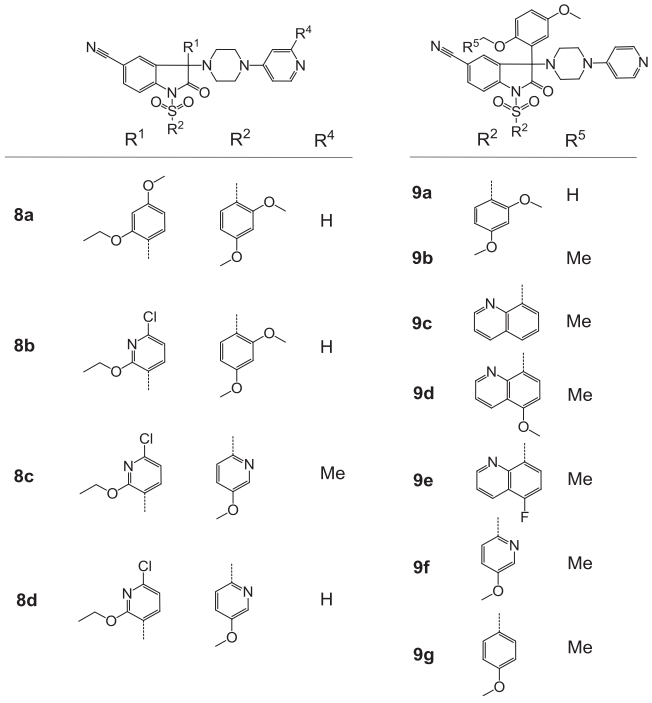

Fig. 6. Derivatives **8a–d** & **9a–g**.

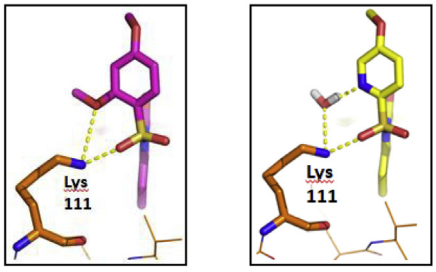

Fig. 7. Compounds **8b** & **8d**, southern substituted phenyl (in stick presentation, magenta and yellow, resp.) in the V1b model. [Residues of protein in stick presentation are within a distance of 6 Å around the molecule. The yellow dotted lines highlight the interactions with the receptor.]

(Table 5, Fig. 6): introduction of an additional methoxy substituent in position 5 (analog **9a**) improved the V1b potency and favored microsomal stability. 2-Methoxy elongation to 2-ethoxy (analog **9b**) didn't impact neither the V1b affinity nor the metabolic stability but favored the V1a selectivity. Despite the sub-optimal OT selectivity, a rat PK was measured for this latter compound: it showed a favorable profile with long terminal half-life, low plasma clearance, moderate oral bioavailability (22%) and good brain penetration (b/p 1.1, Table 6).

Table 6
Pharmacokinetic profile in rat of **(+)-8c**, **9b** & **9c** and SSR149415.

	SSR149415	**(+)-8c**[16]	**9b**[21]	**9c**[21]
MW/clogP	630/0.92	660/3.27	670/3.96	661/3.68
LLE/LigE[6]	7.8/0.28	5.8/0.27	3.7/0.22	4.6/0.24
$t_{1/2}$ (h)[a]	0.5	> 6	3.4	2.4
V_{SS} (L/kg)[a]	2.8	12	2.9	10
Cl_P (L/h/kg)[a]	5.2	0.9	0.7	2.8
F_{oral} (%)[b]	12*	37**	22*	18*
Brain: Plasma Ratio[c]	0.03	1.0	1.1	1.4

[a] After intravenous administration (2 mg kg^{-1}).
[b] After oral administration (*10 mg·kg^{-1}/**5 mg kg^{-1}).
[c] After intraperitoneal administration (10 mg kg^{-1}), calculated based on the AUC in plasma and brain over an 8 h period.

Encouraged by this promising profile, close analogs were prepared (Table 5, Fig. 6).

Replacement of the southern aromatic moiety by substituted 8-quinoline residues afforded single digit nM potency (compounds **9c**, **9d** & **9e**) as already observed for compound **4f** (Table 2). Potency (hV1b) was improved as well as selectivity (> 30-fold towards V1a, OT) but compound **9c** suffered from high microsomal metabolism (h & r, in vitro). Interestingly, the sub-optimal plasma clearance (2.8 l/h/kg) was compensated by a high volume of distribution (10.2 l/kg) so that moderate terminal half-life (2.4 h) and moderate bioavailability (18%) were obtained (rat PK, Table 6). Moreover this compound was characterized by a high brain penetration (b/p 1.4).

Overall, the PK characteristics of compounds **(+)-8c**, **9b** & **9c** represent a considerable improvement over SSR149415, in particular with respect to oral bioavailability, half-life and brain penetration (Table 6).

In the rat forced swimming test, a model with predictive validity for measuring anti-depressant-like effects[19] compound **9c** showed efficacy after intraperitoneal administration of 3 mg/kg (Fig. 8, $p < 0.001$).

In summary, replacing the proline *N*,*N*-dimethylamide moiety of SSR149415 by a substituted piperazine moiety and optimizing the southern and the northern aromatic rings resulted in a new series of potent, selective and highly brain penetrant V1b receptor antagonists with compound **9c** showing efficacy in a rat model of anti-depressant activity. The fact that the PK profile of **9c** was considerably improved over SSR149415 is of particular interest if one considers its higher MW, higher clogP (> 3) and lower LLE[6] (Table 6). This constitutes an unusual optimization approach which takes benefit of the high volume of distribution resulting from the defavorable chemical space (high

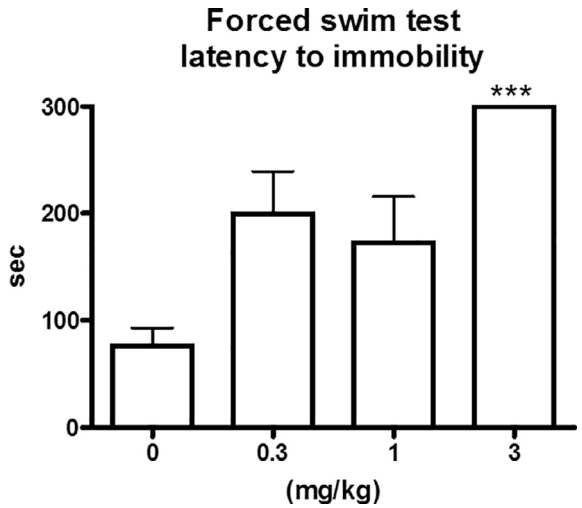

Fig. 8. Effect of compound **9c** in forced swim test in rat.[19,20] **9c** showed efficacy reaching significance at 3 mg/kg. Data are average + SEM.

molecular weight, high lipophilicity) of these V1b antagonists to mitigate the high in vivo plasma clearance.

Declaration of interest

The authors declare the following competing financial interest(s): The authors are current or former employees of AbbVie (or Abbott Laboratories prior to separation), and may own company stocks; the design, study conduct, and financial support for this research were provided by AbbVie/Abbott. AbbVie/Abbott participated in the interpretation of data, review, and approval of the publication.

Acknowledgments

We would like to thank Karl-Peter Orth, Ferdinand Regner and Sonja Triebel and the Analytical Chemistry group in Ludwigshafen.

References

[1]. (a) Serradeil-Le Gal C, Wagnon J, Simiand J, et al. *J Pharmacol Exp Ther.* 2002;300:1122
(b) Griebel G, Simiand J, Serradeil-Le Gal C, et al. *Proc Natl Acad Sci USA.* 2002;99:6370 Other clinical candidates include
(c) ABT-436, Katz DA, Locke C, Greco N, Liu W, Tracy KA. *Brain Behav.* 2017;7:e00628
(d) TASP0233278, TS-121, Iijima M, Yoshimizu T, Shimazaki T, Tokugawa K, Fukumoto K, Kurosu S, Kuwada T, Sekiguchi Y, Chaki S. *Br J Pharmacol.* 2014;171:3511.

[2]. (a) According to information on nelivaptan from Cortellis.com.
(b) Griebel G, Beeske S, Stahl S. *J Clin Psychiatry.* 2012;73:1403

[3]. (a) Hodgson RA, Higgins GA, Guthrie DH, Lu SX, Pond AJ, Mullins DE, Guzzi MF, Parker EM, Varty GB. *Pharmacol Biochem Behav.* 2007;3:431
(b) Kumagai T, Kuwada T, Shibata T, Hayashi M, Fujisawa Y, Sekiguchi Y. *EP 1659121.* 2006
(c) Schönberger M, Leggett C, Kim SW, Hooker JM. *Bioorg Med Chem Lett.* 2010;20:3103.

[4]. Oost T, Backfisch G, Bhowmik S, et al. *Bioorg Med Chem Lett.* 2011;21:3828.

[5]. (a) PDB 4DKL. (b) from Accelrys, San Diego, CA, USA.

[6]. LLE (or LipE) = −log Ki − clogP. (a) Leeson, P. D.; Springthorpe, B. Nat. Rev. Drug Discovery 2007, 6, 881−890. (b) Hopkins, A. L.; Groome, C. R.; Alex, A. Drug Discovery Today 2004, 9, 430−431. LigE (or LE) Bembenek, S.D.; Tounge, B.A.; Reynolds, C.H. Drug Discov. Today 2009, 14, 278.

[7]. hV1b Ki (rac.) = 248 nM.

[8]. The preparation of the building blocks mentioned, typical procedures, and assay setup are described in WO 2008025735, 2008. Chem. Abstr. 2008, 148, 308179 & WO 2008107399, 2008. Chem. Abstr. 2008, 149, 355701, and references cited therein.

[9]. (a) Mongin F, Queguiner G. *Tetrahedron.* 2001;57:4059
(b) Turck A, Ple N, Mongin F, Queguiner G. *Tetrahedron.* 2001;57:4489.

[10]. (a) Tahara A, Saito M, Sugimoto T, Tomura Y, Wada K, Kusayama T, Tsukada J, Ishii N, Yatsu T, Uchida W, Tanaka A. *Brit J Pharmacol.* 1998;125:1463
(b) Strakova Z, Kumar A, Watson AJ, Soloff MS. *Mol Pharmacol.* 1997;51:217
(c) Jasper JR, Harrell CM, O'Brien JA, Pettibone DJ. *Life Sci.* 1995;57:2253
Minimum significant ratio (MSR) parameter that characterizes the reproducibility of potency
Eastwood BJ, Farmen MW, Iversen PW, Craft TJ, Smallwood JK, Garbison KE, Delapp N, Smith GF. *J Biomol Screen.* 2006;11:253.

[11]. Obach S. *Drug Metab Dispos.* 1999;27:1350.

[12]. 3-Pyridin vs 4-pyridin analogs: according to our model[5] the position of the nitrogen (3- or 4-pyridin) is not decisive as the interaction (mainly electrostatic) is mediated by a water molecule (not shown).

[13]. Nassar A-EF, Kamel AM, Clarimont C. *Drug Discov Today.* 2004;9:1020.

[14]. 5-Cl & 5-CN are the only -substituents which allowed retained V1b in vitro potency and selectivity (data not shown).

[15]. The yield (around 40%) as well as the regioisomers ratio **7a**/**7b** (varying from 1:1 to 3:1) are hardly reproducible and highly dependent on the temperature profile of the reaction.

[16]. Optical rotation α = +91° (20 °C, c = 0.7 mg/ml, MeOH, l = 1 dm); separated on Chiracel OD 250x4.6x10mm, eluted with hexane: ethanol:NEt_3 850:150:1 (vol.).

[17]. CYP3A4 IC50 (±)-**8c** 1.2μM, **8d** 0.1μM, (+)-**8c** 2μM - CYP3A4 assay run by co-incubation in human liver microsomes, NADPH & Luciferin BE 50 (0 .03 mg/mL).

[18]. Yanagisawa I, Hirata Y, Ishii Y. *J Med Chem.* 1984;27:849.

[19]. Porsolt RD, Le Pichon M, Jalfre M. *Nature.* 1977;266:730.

[20]. Male Sprague Dawley rats (n = 6) were tested. Animals were trained at day 1 and tested at day 2. Compound 9c was administered 24, 4 and 0.5 h before testing. Floating, swimming and climbing times (**9c**, 3 mg/kg): 159.15 ± 26.10, 12.46 ± 6.63, 125.69 ± 26.88 resp. Nomifensine was used as positive control in this model.

[21]. Analytical data **8c** ESI MS (HRMS, m/z): calcd for $C_{32}H_{31}ClN_7O_5S$ 660.18, found 660.18 [M+]; ^{1}H-NMR (500 MHz, $CDCl_3$) δ (ppm) 8.30 (1H, d), 8.25 (1H, s), 8.15 (2H, m), 8.04 (1H, d), 7.69 (1H, d), 7.34 (1H, d), 7.13 (1H, s), 7.03 (1H, d), 6.44 (1H, s), 6.40 (1H, d), 4.14 (2H, m sym.), 3.88 (3H, s), 2.45 (6H, s), 1.03 (3H, t); **9b** ESI MS (HRMS, m/z): calcd for $C_{35}H_{36}N_5O_7S$ 670.23, found 670.23 [M + H+]; ^{1}H-NMR (600 MHz, Chloroform-d) δ (ppm) 8.25 (m, 2H), 8.14 (d, J = 8.9, 1H), 8.08 (d, J = 8.5, 1H), 7.64 (dd, J = 8.5, 1.8, 1H), 7.44 (d, J = 3.1, 1H), 7.22 (d, J = 1.8, 1H), 6.81 (dd, J = 9.0, 3.1, 1H), 6.74 (d, J = 8.9, 1H), 6.59 (dd, J = 9.0, 2.2, 1H), 6.55 (m, 2H), 6.40 (d, J = 2.3, 1H), 3.89 (m, 1H), 3.82 (s, 6H), 3.74 (m, 1H), 3.65 (s, 3H), 2.95 (m, 8H), 1.12 (t, J = 7.0, 3H); ^{13}C-NMR (151 MHz, $CDCl_3$) δ 171.10, 166.41, 159.08, 154.73, 153.88, 149.86, 149.72, 144.54, 134.49, 133.51, 129.61, 128.81, 126.79, 118.60, 118.50, 114.70, 114.10, 113.65, 113.60, 108.18, 107.92, 104.46, 99.35, 72.29, 69.19, 64.75, 61.89, 55.96, 55.84, 55.77, 46.62, 14.64, 13.95; **9c** ESI MS (HRMS, m/z): calcd for $C_{36}H_{33}N_6O_5S$ 661.22, found 661.22 [M + H+]; ^{1}H-NMR (500 MHz, Chloroform-d) δ (ppm) 8.80 (dd, J = 7.4, 1.4, 1H), 8.70 (dd, J = 4.2, 1.8, 1H), 8.48 (d, J = 8.6, 1H), 8.27 (dd, J = 8.4, 1.8, 1H), 8.18 (m, 2H), 8.13 (dd, J = 8.3, 1.5, 1H), 7.75 (m, 2H), 7.51 (dd, J = 8.3, 4.2, 1H), 7.35 (d, J = 3.1, 1H), 7.18 (d, J = 1.8, 1H), 6.79 (m, 1H), 6.69 (d, J = 9.1, 1H), 6.46 (m, 2H), 3.79 (s, 3H), 3.67 (m, 1H), 3.49 (m, 1H), 2.87 (m, 8H), 0.92 (t, J = 7.0, 3H); ^{13}C-NMR (151 MHz, $CDCl_3$) δ 171.29, 155.54, 153.85, 151.19, 149.51, 145.00, 144.73, 144.17, 136.75, 135.25, 135.04, 134.85, 133.50, 129.15, 128.62, 128.55, 126.41, 125.93, 122.29, 118.53, 116.34, 114.16, 113.61, 113.42, 108.09, 107.47, 69.11, 64.49, 55.74, 46.50, 13.81, 13.70.